

1  
2  
3  
4  
5  
6 Grafting of Oligo(ethylene glycol) Functionalized  
7  
8  
9  
10 Calix[4]arene-tetra-diazonium Salts for Antifouling  
11  
12  
13  
14  
15 Germanium and Gold Surfaces  
16  
17  
18  
19

20 *Pascale Blond,<sup>†,‡</sup> Alice Mattiuzzi,<sup>†,‡</sup> Hennie Valkenier,<sup>⊥</sup> Ludovic Troian-Gautier,<sup>†</sup> Jean-François*  
21 *Bergamini,<sup>§</sup> Thomas Doneux,<sup>Φ</sup> Erik Goormaghtigh,<sup>‡</sup> Vincent Raussens<sup>‡,\*</sup> and Ivan Jabin<sup>†,\*</sup>*

22  
23  
24  
25 <sup>†</sup> Laboratoire de Chimie Organique, Université Libre de Bruxelles (ULB), avenue F. D. Roosevelt  
26 50, CP160/06, B-1050 Brussels, Belgium.  
27  
28  
29

30  
31 <sup>‡</sup> Laboratory for the Structure and Function of Biological Membranes, Center for Structural  
32 Biology and Bioinformatics, Université Libre de Bruxelles (ULB), avenue F. D. Roosevelt 50,  
33 CP206/02, B-1050 Brussels, Belgium.  
34  
35  
36  
37

38  
39 <sup>⊥</sup> Engineering of Molecular NanoSystems, Ecole Polytechnique de Bruxelles, Université Libre de  
40 Bruxelles (ULB), avenue F. D. Roosevelt 50, CP165/64, B-1050 Brussels, Belgium.  
41  
42  
43

44 <sup>§</sup> Université de Rennes 1, Institut des Sciences Chimiques de Rennes (Equipe MaCSE), CNRS,  
45 UMR 6226, Campus de Beaulieu, Bat 10C, 35042 Rennes Cedex, France.  
46  
47  
48

49  
50 <sup>Φ</sup> Chimie Analytique et Chimie des Interfaces, Université Libre de Bruxelles (ULB), Campus de  
51 la Plaine, boulevard du Triomphe, CP255, B-1050 Brussels, Belgium.  
52  
53  
54

55  
56 <sup>‡</sup> X4C, Rue Chêne Bonnet 128, 6110 Montigny-le-Tilleul, Belgium.  
57  
58  
59  
60

## ABSTRACT

Biosensors that can determine protein concentration and structure are highly desired for biomedical applications. For the development of such biosensors, the use of Fourier transformed infra-red (FTIR) spectroscopy with the attenuated internal total reflection (ATR) configuration is particularly attractive but it requires appropriate surface functionalization of the ATR optical element. Indeed, the surface has to specifically interact with a target protein in close contact with the optical element and must display antifouling properties to prevent nonspecific adsorption of other proteins. We here report robust monolayers of calix[4]arenes bearing oEGs chains, which were grafted on germanium and gold surfaces via their tetra-diazonium salts. The formation of monolayers of oEGylated calix[4]arenes was confirmed by AFM, IR and contact angle measurements. The antifouling properties of these modified surfaces were studied by ATR-FTIR spectroscopy and fluorescence microscopy and the non-specific absorption of BSA was found to be reduced by 85% compared to non-modified germanium. In other words, the organic coating by oEGylated calix[4]arenes provides remarkable antifouling properties, opening the way to the design of germanium- or gold-based biosensors.

## INTRODUCTION

Proteins are involved in a very large number of biological processes. Even a small change in their concentration, post-translational modifications, or in their native structure can lead to pathologies.<sup>1</sup> Biosensors that enable fast and selective identification and structural characterization

1  
2  
3 of proteins in complex mixtures represent thus an important target for research.<sup>2,3</sup> A major  
4 challenge in the development of such biosensors is the modification of surfaces by a robust organic  
5 monolayer able to specifically interact with a protein<sup>4</sup> and displaying antifouling properties to  
6 prevent nonspecific adsorption phenomena.  
7  
8  
9  
10

11  
12  
13 In this context, there is an increasing interest in the use of germanium-based surfaces because  
14 this material can be readily used for Fourier transformed infra-red (FTIR) spectroscopy.<sup>5,6,7,8</sup> In  
15 contrast with other detection methods, FTIR spectroscopy allows to simultaneously collect a  
16 wealth of information such as secondary structure and post-translational modifications.<sup>9,10</sup>  
17 Therefore, FTIR spectroscopy with attenuated internal total reflection (ATR) configuration is  
18 currently applied to study mono- and multilayers of bioorganic samples.<sup>11</sup> Because the evanescent  
19 wave propagates outside of the ATR element on a very short distance only, the ATR configuration  
20 allows the detection of analytes in aqueous media when they are brought in close contact with the  
21 optical element. This ATR element could for example be a Ge crystal with the appropriate  
22 geometry. Ge has the advantages over Si (a much more studied element<sup>12</sup>) to have a larger  
23 refractive index (resulting in a better signal-to-noise ratio) and to be transparent in a broader  
24 spectral range, allowing the study of more important chemical groups absorbing between 1400 and  
25 800  $\text{cm}^{-1}$ .  
26  
27  
28  
29  
30  
31  
32  
33  
34  
35  
36  
37  
38  
39  
40  
41  
42  
43

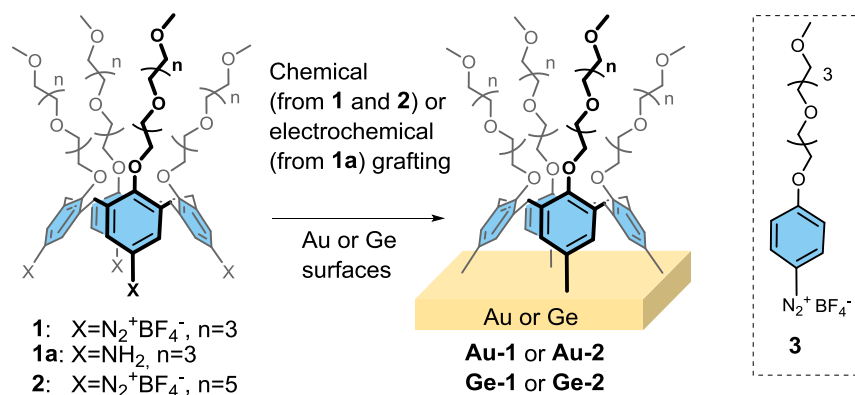
44 Chemisorbed thiols<sup>6,13</sup> and silane derivatives<sup>5,8,14,15</sup> are generally used for the chemical  
45 modification of Ge surfaces. However, the lack of reproducible grafting protocols and of long-  
46 term stability in aqueous media of the obtained monolayers are important limitations of these  
47 methods. In contrast, the reductive grafting of aryldiazonium salts<sup>3,16,17,18</sup> yields stable layers on  
48 Ge.<sup>19,20,21</sup> Nevertheless, this technique generates *in situ* aryl radicals that easily react with the  
49  
50  
51  
52  
53  
54  
55  
56  
57  
58  
59  
60

1  
2  
3 already grafted aryl groups rendering the formation and organization of monolayers difficult to  
4  
5 control.<sup>22,23</sup>  
6  
7

8  
9 In this regard, we have recently developed a general strategy for the formation of robust,  
10  
11 homogeneous and well-organized organic monolayers on various surfaces thanks to the use of  
12  
13 calix[4]arene-tetra-diazonium salts.<sup>24,25,26</sup> These compounds can be electrochemically or  
14  
15 chemically reduced to produce aryl radicals that can be grafted *via* multiple covalent bonds. The  
16  
17 structure and geometry of the calix[4]arenes do not allow any additional grafting, preventing the  
18  
19 formation of multilayers. Furthermore, when grafting calix[4]arenes functionalized at the small  
20  
21 rim with for instance appending COOH groups, the resulting calixarene layer can be further post-  
22  
23 functionalized under mild conditions by various chemical species.<sup>24</sup> An additional feature, in  
24  
25 contrast to all the other known methods, is the preparation of binary monolayers of controlled  
26  
27 composition in a single step from the grafting of binary mixtures of calix[4]arene-tetra-diazonium  
28  
29 salts.<sup>27,28</sup>  
30  
31  
32  
33  
34

35  
36 Regarding the nonspecific adsorption of proteins and biomacromolecules, this is typically  
37  
38 prevented by surface modification with small shielding molecules or polymers. Coatings based on  
39  
40 oligo(ethylene glycol) (oEG), polysaccharides, zwitterionic compounds or perfluoroalkyls are  
41  
42 some examples.<sup>29,30,31,32,33,34</sup> As oEGs are nontoxic and nonimmunogenic, they are widely used in  
43  
44 medical applications.<sup>35,36,37,38</sup> The dominant way through which proteins adhere to surfaces is by  
45  
46 hydrophobic effect.<sup>39,40</sup> Uncharged oEGylated surfaces interact with water molecules, preventing  
47  
48 this hydrophobic effect and thus effectively shielding the surface from protein fouling. It is  
49  
50 noteworthy that the grafting of antifouling coatings on Ge has been scarcely reported.<sup>14,41</sup>  
51  
52  
53  
54  
55  
56  
57  
58  
59  
60

In order to develop a new ATR device suitable for biosensing applications, we have investigated the grafting on Ge of a robust monolayer of calix[4]arenes decorated with multiple oEGs arms. For this, calix[4]arene-tetra-diazonium salts bearing oEGs substituents of different lengths (**1** and **2**) and a reference compound **3**<sup>42</sup> were synthesized (Scheme 1). The feasibility of the grafting was first evaluated on standard gold surfaces through previously developed electrochemical and chemical grafting processes.<sup>26</sup> As Ge is a semi-conducting surface, the conventional electrochemical grafting process is not appropriate and thus only the chemical process was then used. Finally, the antifouling properties of the surfaces that were modified with oEGylated calixarenes were evaluated by FTIR spectroscopy and confocal laser scanning fluorescence microscopy upon exposure to proteins.



**Scheme 1.** Chemical grafting of calix[4]arenes **1** and **2** or electrochemical grafting of **1a**. Inset: structure of reference diazonium salt **3**. Note that the representation of the grafted calixarene does not necessarily imply that its four aryl units are linked to the surface.

## EXPERIMENTAL SECTION

1  
2  
3 **Chemicals and materials.** All solvents and reagents were at least of reagent grade quality and  
4 were purchased either from Alfa Aesar, Sigma-Aldrich, TCI, Roth or Acros organics. All reactions  
5 were performed under an inert atmosphere. Reactions were magnetically stirred and monitored by  
6 thin layer chromatography using Merck-Kieselgel 60F254 plates. Flash chromatography was  
7 performed with silica gel 60 (particle size 35-70  $\mu\text{m}$ ) supplied by Merck. Anhydrous DMF was  
8 obtained from Acros organics. Anhydrous THF was obtained from distillation on  
9 Na/benzophenone. Ultrapure water was obtained via a Millipore Milli-Q system (18.2 M $\Omega$  cm).  
10 The fluorescent FITC-BSA (fluorescein isothiocyanate BSA conjugate) was purchased from  
11 Sigma-Aldrich as well as the BSA used for ATR-FTIR spectroscopy experiments. Gold-coated  
12 silicon wafer (1000  $\text{\AA}$  layer thickness) was purchased from Sigma-Aldrich. Both sides polished  
13 germanium squares (10 x 10 x 0.5 mm) and germanium single-crystal triangular prisms (base 6.8  
14 mm x 45 mm length and an internal incident angle of 45 $^\circ$ ) were purchased from ACM (France).  
15  
16  
17  
18  
19  
20  
21  
22  
23  
24  
25  
26  
27  
28  
29

30 **Caution!** Although we have not encountered any problem, it is noted that diazonium salts  
31 derivatives are potentially explosive and should be handled with appropriate precautions.  
32  
33

34 Both calix[4]arene-tetra-oEGs **1** and **2** were prepared following the same strategy. The detailed  
35 synthesis of compound **1** (Scheme 2) is given here, while details for the compounds **2** and **3** are  
36 reported in the SI.  
37  
38  
39  
40  
41

42 **15,35,55,75-tetra-tert-butyl-12,32,52,72-tetrakis(2-(2-methoxyethoxy)ethoxy)-1,3,5,7(1,3)-**  
43 **tetrabenzenacyclooctaphane 6.** Commercial *p*-<sup>t</sup>Bu-calix[4]arene (2.0 g, 3.1 mmol) was dissolved  
44 in dry DMF (50 mL). NaH (60% dispersion in oil, 0.840 g, 21.0 mmol) and 2,5,8,11-  
45 tetraoxatridecan-13-yl 4-methylbenzenesulfonate **4** (7.6 g, 21.0 mmol) were added and the reaction  
46 mixture was stirred for 24 hours at 75 $^\circ\text{C}$  under inert atmosphere. The reaction mixture was then  
47 brought to room temperature and quenched dropwise with 5 mL of HCl (0.5 M). The mixture was  
48  
49  
50  
51  
52  
53  
54  
55  
56  
57  
58  
59  
60

1  
2  
3 then concentrated under reduced pressure. The resulting oil was dissolved in CH<sub>2</sub>Cl<sub>2</sub> (200 mL),  
4 the organic layer was washed with H<sub>2</sub>O (3 x 150 mL) and the combined aqueous layers were  
5 extracted with CH<sub>2</sub>Cl<sub>2</sub> (300 mL). The combined organic layers were concentrated under reduced  
6 pressure. The crude oil was purified by flash chromatography on silica gel (EtOAc/MeOH =  
7 85:15). The oil was washed with H<sub>2</sub>O to yield the compound **6** as a yellow oil (4.2 g, 3.0 mmol,  
8 96%).  
9

10  
11  
12 <sup>1</sup>H NMR (300 MHz, CDCl<sub>3</sub>, 298K), δ (ppm): 1.06 (s, 36H), 3.09 (d, *J* = 12 Hz, 4H), 3.37 (s,  
13 12H), 3.49-3.71 (m, 48H), 3.93 (t, *J* = 4.5 Hz, 8H), 4.09 (t, *J* = 4.5 Hz, 8H), 4.41 (d, *J* = 12 Hz,  
14 4H), 6.75 (s, 8H). <sup>13</sup>C NMR (100 MHz, CDCl<sub>3</sub>, 298K), δ (ppm): 31.2, 31.6, 33.9, 59.2, 70.5, 70.6,  
15 70.6, 70.7, 70.8, 70.8, 72.1, 73.0, 125.1, 133.9, 144.7, 153.4. FTIR, ν (cm<sup>-1</sup>): 3412, 2952, 2921,  
16 2899, 2867, 1644, 1480 1457, 1392, 1361, 1300, 1249, 1199, 1107, 1062, 1027, 944, 869. HRMS:  
17 calcd. for C<sub>80</sub>H<sub>128</sub>O<sub>20</sub> (M+H)<sup>+</sup> 1409.91 found 1409.91.  
18

19  
20  
21 **15,35,55,75-tetra-nitro-12,32,52,72-tetrakis(2-(2-methoxyethoxy)ethoxy)-1,3,5,7(1,3)-**  
22 **tetrabenzenacyclooctaphane 8**. Note that compound **8** was already described in the literature<sup>43</sup>  
23 but is here prepared *via* another synthetic strategy. Calix[4]arene-tetra-oEG<sub>4</sub> **6** (4.2 g, 3.0 mmol)  
24 was dissolved in CH<sub>2</sub>Cl<sub>2</sub> (100 mL). A mixture of glacial CH<sub>3</sub>COOH/fuming HNO<sub>3</sub> (1:1) (22 mL)  
25 was added at 0°C and the reaction mixture was stirred for 5 hours at room temperature. The  
26 reaction mixture was concentrated under reduced pressure. The resulting oil was dissolved in  
27 CH<sub>2</sub>Cl<sub>2</sub> (100 mL), the organic layer was washed with H<sub>2</sub>O (3 x 70 mL) and the combined aqueous  
28 layers were extracted with CH<sub>2</sub>Cl<sub>2</sub> (150 mL). The combined organic layers were concentrated  
29 under reduced pressure. The crude oil was purified by flash chromatography on silica gel  
30 (DCM/Acetone = 65:35) to yield compound **8** as a yellow oil (2.5 g, 1.8 mmol, 61%).  
31  
32  
33  
34  
35  
36  
37  
38  
39  
40  
41  
42  
43  
44  
45  
46  
47  
48  
49  
50  
51  
52  
53  
54  
55  
56  
57  
58  
59  
60

<sup>1</sup>H NMR spectrum of compound **8** is in accordance with the one reported in the literature.<sup>43</sup> <sup>1</sup>H NMR (300 MHz, CDCl<sub>3</sub>, 298K), δ (ppm): 3.33-3.44 (m, 16H), 3.48-3.63 (m, 48H), 3.80 (t, *J* = 4.5 Hz, 8H), 4.24 (t, *J* = 4.5 Hz, 8H), 4.65 (d, *J* = 12 Hz, 4H), 7.58 (s, 8H).

**12,32,52,72-tetrakis(2-(2-methoxyethoxy)ethoxy)-1,3,5,7(1,3)-tetrabenzenacyclooctaphane-15,35,55,75-tetraamine 1a.** Note that compound **1a** was already described in the literature<sup>43</sup> but is here prepared *via* another synthetic strategy. Calix[4]arene-tetra-NO<sub>2</sub>-tetra-oEG<sub>4</sub> **8** (0.901 g, 0.660 mmol) and Pd/C (53 mg, 0.498 mmol) were suspended in EtOH (18 mL). Hydrazine hydrate (3 mL, 61.8 mmol) was added dropwise and the reaction mixture was stirred for 15 hours at reflux. The reaction mixture was filtered on Celite and the Celite was washed with EtOH and CH<sub>2</sub>Cl<sub>2</sub>. The filtrate was concentrated under reduced pressure to yield the compound **1a** as a yellow oil (0.798 g, 0.641 mmol, 97%).

<sup>1</sup>H NMR spectrum of compound **1a** is in accordance with the one reported in the literature.<sup>43</sup> <sup>1</sup>H NMR (300 MHz, CD<sub>3</sub>OD, 298K), δ (ppm): 2.94 (d, *J* = 13 Hz, 4H), 3.35 (s, 12H), 3.48-3.70 (m, 48H), 3.89 (t, *J* = 5 Hz, 8H), 4.03 (t, *J* = 5 Hz, 8H), 4.40 (d, *J* = 13 Hz, 4H), 6.17 (s, 8H).

**12,32,52,72-tetrakis(2-(2-methoxyethoxy)ethoxy)-1,3,5,7(1,3)-tetrabenzenacyclooctaphane-15,35,55,75-tetrakis(diazonium) 1.** Calix[4]-tetra-aniline-tetra-oEG<sub>4</sub> **1a** (50 mg, 0.040 mmol) was solubilized in dry acetonitrile (0.5 mL). At -40°C, NOBF<sub>4</sub> (46 mg, 0.400 mmol) was added and the reaction mixture was stirred for 2 hours at -40°C under inert atmosphere. The reaction mixture was concentrated under reduced pressure at room temperature to yield the compound **1** as a yellow/orange oil. Due to the well-known low stability of diazonium groups, compound **1** was used without further purification for the grafting experiments.

HRMS analysis was not performed because of the low stability of compound **1** against temperature.



<sup>1</sup>H NMR (600 MHz, CD<sub>3</sub>CN, 298K), δ (ppm): 3.30 (s, 12H), 3.43-3.59 (m, 48H), 3.78 (d, *J* = 14 Hz, 4H), 3.84 (br t, 8H), 4.49 (br t, 8H), 4.72 (d, *J* = 14 Hz, 4H), 8.02 (br s, 8H). <sup>13</sup>C NMR (150 MHz, CD<sub>3</sub>CN, 298K), δ (ppm): 31.0, 58.9, 70.4, 70.7, 70.7, 70.9, 71.0, 71.0, 72.5, 77.5, 107.7, 135.0, 138.7, 168.7. FTIR, ν (cm<sup>-1</sup>): 3083, 2942, 2883, 2267, 1571, 1443, 1355, 1293, 1264, 1096, 1025, 922, 846.

**Electrochemical grafting strategy.** Electrochemical measurements were conducted in a three-electrode cell using a Ag|AgCl saturated KCl electrode as reference electrode, a large area platinum foil as counter electrode, and a polycrystalline gold disk (1.6 mm in diameter, from Bioanalytical Systems) as working electrode, all connected to an Autolab PGSTAT30 (Metrohm Autolab) potentiostat equipped with a ScanGen module.

Gold electrodes were first polished with alumina paste (1 μm particles) and sonicated in ultrapure water for 10 minutes before being dried under a flux of nitrogen. The diazonium salt **1** was prepared *in situ* in 0.5 M aqueous HCl in the presence of NaNO<sub>2</sub> (8 eq.) from the corresponding calix[4]-tetra-aniline **1a** (1.5 mM). The gold substrate was functionalized through the reduction of the *in situ* generated diazonium cations by six voltammetric cycles, the potential being swept between +0.5 V and -0.4 V versus Ag|AgCl electrode. Once the grafting was achieved, the surfaces were thoroughly rinsed with ultrapure water and sonication was applied for 10 minutes.

**Chemical grafting strategy. Caution!** Piranha solution is a very strong oxidant and should be handled very carefully. Gold surfaces were first immersed in a piranha solution (H<sub>2</sub>SO<sub>4</sub>/H<sub>2</sub>O<sub>2</sub> 3:1) for 10 minutes and sonicated for 5 minutes. They were subsequently washed with concentrated sulphuric acid and with ultrapure water and then dried under argon atmosphere. Germanium surfaces were first immersed in ultrapure water and then in ethanol; sonication was applied each

1  
2  
3 time for 5 minutes. They were then rinsed with Et<sub>2</sub>O and dried under argon atmosphere. The  
4  
5 surfaces were dipped in a 5 mM solution of the diazonium salt (**1-3**) in aqueous 0.1 M sodium  
6  
7 hydroxide for 2 hours, without stirring in order to avoid any mechanical damage of the surface by  
8  
9 the magnetic stirrer bar (a minimal volume of solution is used). Once the grafting was achieved,  
10  
11 all the surfaces were thoroughly washed with ultrapure water and then acetonitrile. Sonication was  
12  
13 applied each time for 5 minutes. The surfaces were then dried under argon flow.  
14  
15

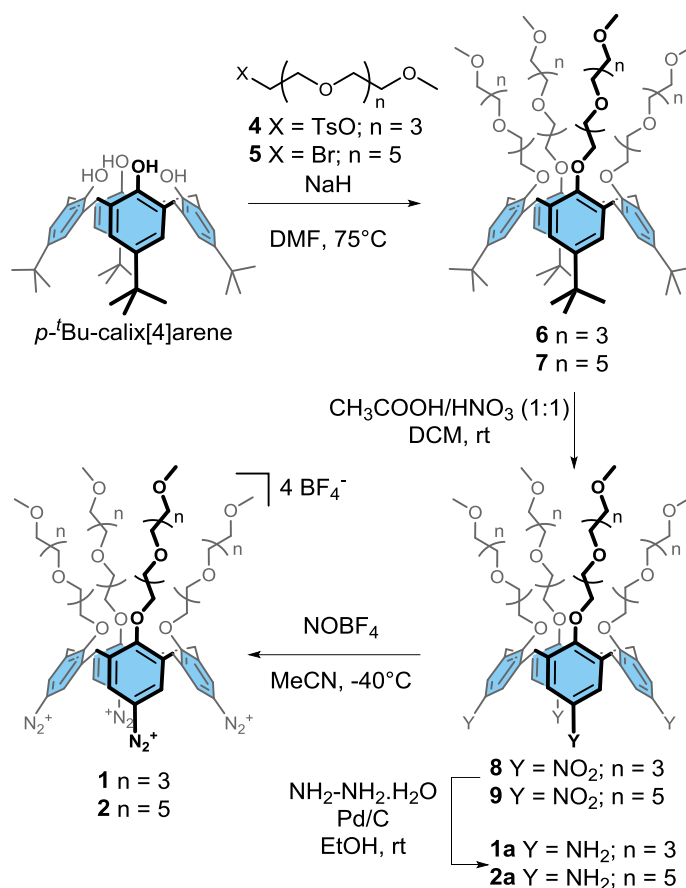
16  
17 **ATR-FTIR** spectra were recorded at 22°C on a Bruker Equinox 55 FTIR spectrophotometer  
18  
19 equipped with a liquid nitrogen-cooled mercury-cadmium-telluride (MCT) detector. The  
20  
21 spectrophotometer was continuously purged with dried air. The target chemicals were deposited  
22  
23 in solution on a germanium single-crystal internal reflection element (triangular prism of 6.8 x 45  
24  
25 mm, with an internal incidence angle of 45°) and the solvent was removed with a flow of nitrogen  
26  
27 gas. The spectra from the grafted monolayer were obtained following the chemical grafting of the  
28  
29 calix[4]arene target directly on the germanium internal reflection element. In each case, bare  
30  
31 germanium was used for the background spectrum. The nonspecific adsorption experiment was  
32  
33 measured in a flow-through cuvette with a 100 µg/mL solution of BSA in phosphate buffer media  
34  
35 in D<sub>2</sub>O (PBS-D<sub>2</sub>O) and a flow rate of 10 µL/min. Opus software (4.2.37) was used to record 128  
36  
37 scans with a nominal resolution of 2 cm<sup>-1</sup> for Figures 1 and S54 and 64 scans with a nominal  
38  
39 resolution of 4 cm<sup>-1</sup> for Figures 2, S55 and S56. Data were processed and analysed using the home-  
40  
41 written Kinetics package in Matlab R2013a by subtraction of water vapor, baseline correction,  
42  
43 apodization at 16 cm<sup>-1</sup>.  
44  
45  
46  
47  
48

49 **Confocal Laser Scanning Fluorescence Microscopy:** fluorescence images were recorded with  
50  
51 a Nikon Ti-Eclipse inverted microscope, equipped with a laser emitting at 488 nm. The emitted  
52  
53 light was collected in the epi-fluorescence mode and a dichroic mirror was employed to select  
54  
55  
56  
57  
58  
59  
60

1  
2  
3 wavelengths shorter than 540 nm. A bandpass emission filter (515–530 nm), matching well the  
4 emission spectrum of fluorescein, was placed in front of the photo-multiplier tube. A 10×  
5 magnification objective (NA = 0.30, working distance 16 mm) was employed. The images were  
6 processed with the software ImageJ.  
7  
8  
9  
10  
11  
12  
13  
14

## 15 RESULTS AND DISCUSSION

16  
17  
18 Both calix[4]arene-tetra-oEGs **1** and **2** were prepared following the strategy developed for other  
19 calix[4]arene-tetra-diazonium salts (Scheme 2).<sup>24,26</sup> First, a tetra O-alkylation of *p*-<sup>t</sup>Bu-  
20 calix[4]arene constrained the macrocycle in a cone conformation and allowed the introduction of  
21 the oEGs arms on the small rim. Then, a sequence of ipso-nitration / reduction afforded the tetra-  
22 anilines **1a** and **2a** in respectively 57 % and 52 % overall yields from *p*-<sup>t</sup>Bu-calix[4]arene. Finally,  
23 a diazotation reaction yielded target diazonium salts **1** and **2** whose structures were clearly  
24 confirmed by 1D and 2D NMR spectroscopy. Grafting experiments were performed on gold and  
25 germanium surfaces with both calix[4]arenes **1** and **2** as well as with the reference compound **3** for  
26 comparison (Scheme 1).  
27  
28  
29  
30  
31  
32  
33  
34  
35  
36  
37  
38  
39  
40  
41  
42  
43  
44  
45  
46  
47  
48  
49  
50  
51  
52  
53  
54  
55  
56  
57  
58  
59  
60



33 **Scheme 2.** Synthesis of calix[4]arene-tetra-oEG<sub>n</sub>-tetra-diazonium salts **1** and **2**.

34  
35  
36  
37  
38 Similarly to previously reported calixarenes,<sup>26</sup> grafting of the new oEGylated calixarenes was  
39 first evaluated on a gold substrate, using calix[4]-tetra-aniline precursor **1a**, from which the  
40 corresponding tetra-diazonium salt **1** was prepared *in situ* by adding an excess of NaNO<sub>2</sub> in acidic  
41 conditions. Reduction of the diazonium cations was performed by six voltammetric cycles. The  
42 density of the electrografted layer was characterized by analyzing its blocking property towards  
43 the electrochemical response of the redox probe Fe(CN)<sub>6</sub><sup>3-/4-</sup>.<sup>24</sup> Complete inhibition of the  
44 electrochemical response was found, indicating that a dense organic layer had been formed at the  
45 electrode surface (Figure S51).  
46  
47  
48  
49  
50  
51  
52  
53  
54  
55  
56  
57  
58  
59  
60

1  
2  
3 Having found that the electrochemical grafting methodology was applicable to the newly  
4 synthesized calix[4]arene-tetra-oEGs, we subsequently undertook the chemical grafting of the  
5 diazonium salts (**1-3**) on Au and Ge substrates. The previously reported protocols for the grafting  
6 of aryl diazonium salts on Ge in organic solvents requires an oxide-free Ge surface obtained by  
7 treatment with an aqueous HF solution.<sup>19,20,21</sup> Here, the grafting procedure on Ge substrate was  
8 performed in a basic aqueous solution and involved the *in situ* formation of diazoates.<sup>44,45,46</sup> Under  
9 these aqueous conditions, the laborious and hazardous pre-treatment with aqueous HF is not  
10 needed, as the Ge oxide at the surface is water soluble.<sup>47</sup> The chemical grafting of diazonium salts  
11 **1, 2** and **3** was performed upon immersion of the Au and Ge substrates in an aqueous 0.1 M NaOH  
12 solution containing 5 mM of the desired diazonium salt for 2 hours. This procedure afforded gold  
13 surfaces **Au-1**, **Au-2** and **Au-3** and germanium surfaces **Ge-1** and **Ge-2** (Scheme 1). Each grafting  
14 experiment was repeated at least three times to assess the reproducibility.

15  
16  
17 All these modified surfaces were then characterized by contact angle measurements and the  
18 results were compared to those obtained with bare surfaces (*i.e.*, surfaces that were treated  
19 similarly to the modified ones but in the absence of the diazonium salt). Contact angles of  $62 \pm 9^\circ$   
20 and  $30 \pm 10^\circ$  were obtained respectively for bare Au and Ge substrates (Table 1). For all the  
21 modified oEGylated surfaces, the contact angle was found to be *ca.*  $56^\circ$ . These results clearly  
22 confirm the presence of the oEG layer on all the modified surfaces and highlight the reproducibility  
23 of the grafting process. Furthermore, the value of *ca.*  $56^\circ$  is in agreement with those found in  
24 literature for oEGylated surfaces.<sup>48</sup>

25  
26  
27 **Table 1.** Contact angle measurements and thickness estimations of the grafted organic layers.

Contact angle <sup>a</sup> (°)	Thickness <sup>b</sup> (nm)
--------------------------------	-----------------------------

Bare Au <sup>c</sup>	62 ± 9	-
<b>Au-1</b>	55 ± 5	2.4 ± 0.4
<b>Au-2</b>	56 ± 4	n.d. <sup>d</sup>
<b>Au-3</b>	56 ± 7	19.0 ± 1.0
Bare Ge <sup>c</sup>	30 ± 10	-
<b>Ge-1</b>	56 ± 1	3.0 ± 0.3
<b>Ge-2</b>	56 ± 3	n.d. <sup>d</sup>

<sup>a</sup> Average values obtained by multiple analyses repeated on several surfaces. <sup>b</sup> Determined by AFM measurement (see text). <sup>c</sup> The bare surfaces were treated similarly to the modified ones but in the absence of the diazonium salt. <sup>d</sup> n.d.: not determined.

Atomic Force Microscopy (AFM) measurements were performed on the surfaces **Au-1**, **Au-3**, **Ge-1** and on the bare gold and germanium substrates. All the modified surfaces exhibited a surface topography similar to that of the corresponding bare substrate, indicating a thin uniform deposit on the surface (Figure S52 and S53). Next, thicknesses of the organic layers were estimated in contact mode through scratching experiments. The AFM tip was used to scratch a square area on the modified samples by exercising a force sufficient to remove the organic part without damaging the substrate. Using the height difference between both areas of the surface profile (Figure S52 and S53), thicknesses of the organic layer of 2.4 and 3.0 nm were found for **Au-1** and **Ge-1** respectively (Table 1). These values correspond well with the height of the calix[4]arene-tetra-oEG<sub>4</sub> structure (*ca.* 2.2 nm estimated from MM2 energy minimizations with ChemBio3D software), suggesting that a monolayer of grafted calix[4]arene-tetra-oEGs **1** was obtained on gold and germanium. In the case of the control surface **Au-3**, a thickness of 19.0 nm was estimated, clearly indicating the formation of multilayers. This result highlights the crucial role played by the calixarene structure in the formation of monolayers.

The germanium surfaces **Ge-1** and **Ge-2** were then analyzed by ATR-FTIR spectroscopy. For comparison, the IR absorbance spectra of compounds **1**, **2** and their corresponding anilines **1a** and **2a** were recorded (Figures 1 and S54). Typical bands belonging to the calix[4]arene core and oEG groups were observed both for the compounds and the corresponding monolayers. The asymmetric COC stretching from the oEG chains around 1100  $\text{cm}^{-1}$  is clearly visible in all spectra. Other bands can be attributed to the calix[4]arene moieties such as the symmetric  $\text{COC}_{\text{Ar}}$  stretching around 1050 – 1020  $\text{cm}^{-1}$  and the aromatic ring stretching around 1460  $\text{cm}^{-1}$ . The IR results thus clearly confirm the grafting of calixarenes **1** and **2** on Ge.

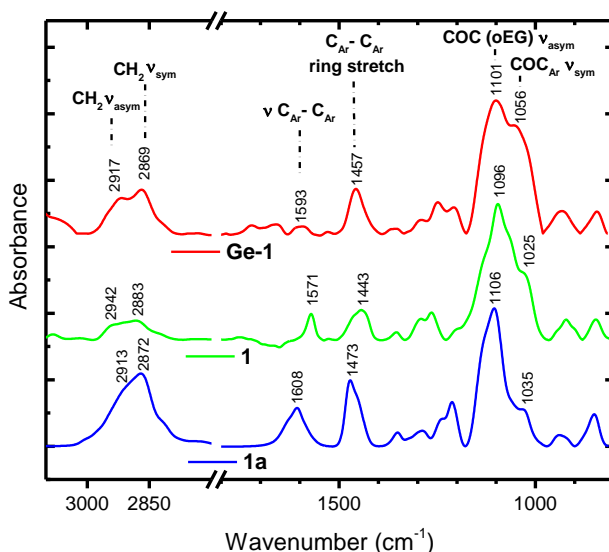


**Figure 1.** ATR-FTIR absorption spectra from 3100-2700 and 1800-800  $\text{cm}^{-1}$  of modified surface **Ge-1** (red), calix[4]arene-tetra-diazonium salt **1** (green) and calix[4]-tetra-aniline **1a** (blue).

The nonspecific adsorption of proteins on bare Ge and on oEGylated Ge substrates was monitored by ATR-FTIR spectroscopy. Surfaces **Ge-1** and **Ge-2** were compared to evaluate the influence of the chain length of oEGs on the protein adsorption. A flow-through cuvette with a

1  
2  
3 solution of bovine serum albumin (BSA, 100  $\mu\text{g/mL}$ ) in phosphate buffer media in  $\text{D}_2\text{O}$  (PBS-  
4  $\text{D}_2\text{O}$ ) at  $22^\circ\text{C}$  was used to analyze the nonspecific binding of BSA on the surfaces. BSA is used as  
5  
6 model protein in many investigations because it is one of the most abundant proteins found in  
7  
8 blood and it adheres very well to surfaces. First, the stability of the calixarene layer under the study  
9  
10 conditions was evaluated through exposure of the surface **Ge-1** to a flow (10  $\mu\text{L/min}$ ) of PBS- $\text{D}_2\text{O}$   
11  
12 buffer during 16 h. The decomposition of the organic layer should give rise to the appearance of  
13  
14 negative absorbance bands in the regions where the calixarene signals are located (*e.g.*, at 1100  
15  
16  $\text{cm}^{-1}$ ). This was not observed, indicating that the calix[4]arene monolayer is stable under aqueous  
17  
18 conditions for at least 16 hours (Figure S55). The surfaces **Ge-1** and **Ge-2** were then placed under  
19  
20 a flow (10  $\mu\text{L/min}$ ) of the PBS- $\text{D}_2\text{O}$  medium for 10 min in order to reach an equilibrium state  
21  
22 under aqueous conditions. The flow was then switched to the solution of BSA in PBS- $\text{D}_2\text{O}$  for 16  
23  
24 hours and finally back to PBS- $\text{D}_2\text{O}$  for 5 hours. Infrared spectra were recorded every minute for  
25  
26 the first 20 minutes and then every 10 minutes till the end of the experiment. Adsorbed BSA was  
27  
28 characterized by two bands whose intensities were increasing over time: the amide-I' at 1640  $\text{cm}^{-1}$ ,  
29  
30 which is mainly associated with the C=O(ND) stretching vibrations and the amide-II' at 1450  
31  
32  $\text{cm}^{-1}$ , which results mainly from in plane ND bending vibrations (Figure 2a and S56). The integral  
33  
34 of the amide-I' band at 1640  $\text{cm}^{-1}$  was calculated for each spectrum. The graph shows that the  
35  
36 binding of BSA to surfaces **Ge-1** and **Ge-2** is reduced by more than 85% in comparison to bare Ge  
37  
38 (Figure 2b). No difference was found between **Ge-1** and **Ge-2**, showing that an oEG length of four  
39  
40 on the calix[4]arenes is sufficient for the effective prevention of nonspecific protein adsorption on  
41  
42 Ge. Such an efficiency in the reduction of nonspecific adsorption has been reported scarcely and,  
43  
44 in the case of the previous systems, either a very thick coverage was necessary (*e.g.*, polymer  
45  
46 brushes)<sup>48,49</sup> or a limited stability was observed.<sup>36</sup>  
47  
48  
49  
50  
51  
52  
53  
54  
55  
56  
57  
58  
59  
60



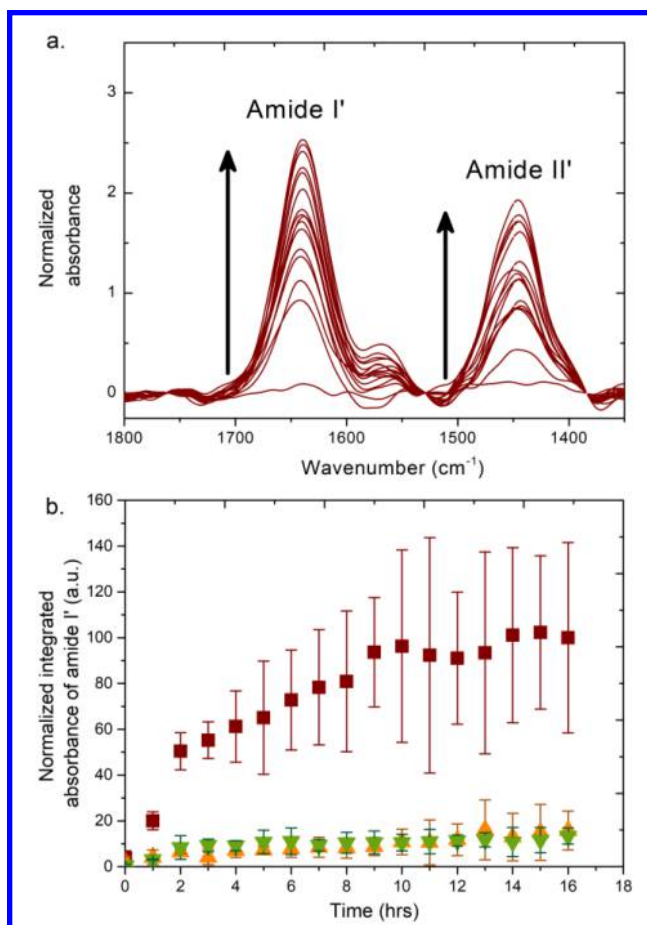
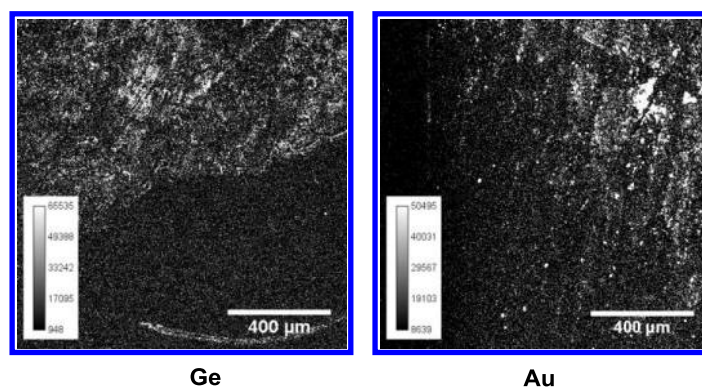


**Figure 2.** (a) ATR-FTIR absorption spectra from 1800-1350  $\text{cm}^{-1}$  reported for every hour during the BSA nonspecific adsorption experiment on bare Ge. (b) Normalized adsorption of BSA on bare Ge substrate (dark red ■), Ge-1 (orange ▲) and Ge-2 (green ▼). The error bars correspond to the standard deviation obtained from two or three independent measurements.

The nonspecific adsorption of proteins was also evaluated by confocal laser scanning fluorescence microscopy. A defined area of Au and Ge surfaces was first modified with the calix[4]arene-tetra-oEG<sub>4</sub> **1**, the surfaces were then submerged in a 100  $\mu\text{g}/\text{mL}$  solution of fluorescent FITC-BSA in PBS buffer for 6 hours, followed by rinsing in PBS buffer for 16 hours. The resulting fluorescence images are shown in Figure 3. On both images, two areas can be clearly

1  
2  
3 distinguished: the unmodified one serving as control (top) and the one modified with the  
4 calix[4]arene (bottom). On the modified zone, the fluorescence is significantly decreased, showing  
5 a drastic reduction of the nonspecific adsorption of BSA. This result is not quantitative, but gives  
6 a good indication of the remarkable antifouling character of the modified surfaces.  
7  
8  
9  
10  
11  
12



26 **Figure 3.** Fluorescence images acquired on gold and germanium surfaces that were partially  
27 modified with the calix[4]arene-tetra-oEG<sub>4</sub> **1** and subsequently immersed in a 100 μg/mL solution  
28 of fluorescently labelled BSA in PBS buffer for 6 hours.  
29  
30  
31  
32  
33  
34

## 35 CONCLUSIONS

36  
37  
38  
39 In conclusion, we have developed a reproducible procedure for the grafting of thin and robust  
40 organic monolayers of calix[4]arene-tetra-oEGs on Ge and Au that do not require any laborious or  
41 dangerous pre-treatment. The significant antifouling properties of these monolayers were  
42 demonstrated. The nonspecific adsorption of proteins was decreased by more than 85% compared  
43 to bare Ge. Such an efficiency is unique if we consider the thickness (*ca.* 3 nm) and the high  
44 stability of the calixarene layer. The modified Ge surfaces thus constitute promising devices for  
45 the development of ATR-FTIR-biosensors. Current developments in our laboratories are directed  
46  
47  
48  
49  
50  
51  
52  
53  
54  
55  
56  
57  
58  
59  
60

1  
2  
3 toward the grafting of calix[4]arene-tetra-oEGs with terminal post-functionalizable groups (*e.g.*  
4  
5 COOH, azide or alkyne groups) that can serve for the controlled immobilization of proteins.  
6  
7  
8  
9  
10

## 11 ASSOCIATED CONTENT

### 12 13 14 15 **Supporting Information**

16  
17  
18 The Supporting Information is available free of charge on the ACS Publications website at DOI:.

19  
20  
21 Detailed procedure for the preparation and characterization of the synthesized compounds, NMR  
22  
23 spectra, AFM results, and additional FTIR experiments. This material is available free of charge  
24  
25 via the Internet at <http://pubs.acs.org>.  
26  
27  
28  
29  
30

## 31 AUTHOR INFORMATION

### 32 33 34 **Corresponding Authors**

35  
36  
37 \*E-mail: [ijabin@ulb.ac.be](mailto:ijabin@ulb.ac.be); [vrauss@ulb.ac.be](mailto:vrauss@ulb.ac.be)  
38  
39

### 40 **ORCID**

41  
42 Pascale Blond: 0000-0001-8515-1737

43  
44 Alice Mattiuzzi: 0000-0002-3784-8449

45  
46 Hennie Valkenier: 0000-0002-4409-0154

47  
48 Ludovic Troian-Gautier: 0000-0002-7690-1361

49  
50 Thomas Doneux: 0000-0002-9082-8826

51  
52 Erik Goormaghtigh: 0000-0002-2071-2262  
53  
54  
55  
56  
57  
58  
59  
60

1  
2  
3 Vincent Raussens: 0000-0002-7507-1845  
4

5 Ivan Jabin: 0000-0003-2493-2497  
6  
7  
8  
9

## 10 Notes

11  
12 The authors declare no competing financial interest.  
13  
14  
15  
16

## 17 ACKNOWLEDGMENT

18  
19 The “Actions de Recherches Concertées” of the Fédération Wallonie-Bruxelles and the ULB  
20  
21 (Ph.D. grant to P.B.) are acknowledged for financial support.  
22  
23  
24  
25

## 26 REFERENCES

27  
28  
29  
30  
31  
32 <sup>1</sup> Gestwicki, J. E.; Garza, D. Chapter 10 - Protein Quality Control in Neurodegenerative Disease.  
33 In *Progress in Molecular Biology and Translational Science*, Teplow, D. B., Ed. Academic Press:  
34 **2012**, Vol. 107, pp 327-353.  
35

36  
37  
38 <sup>2</sup> Leech, D. Affinity Biosensors. *Chem. Soc. Rev.* **1994**, *23*, 861-878.  
39  
40

41  
42 <sup>3</sup> Cao, C.; Zhang, Y.; Jiang, C.; Qi, M.; Liu, G. Advances on Aryldiazonium Salt Chemistry  
43 Based Interfacial Fabrication for Sensing Applications. *ACS Appl. Mater. Inter.* **2017**, *9*, 5031-  
44  
45 5049.  
46  
47

48  
49 <sup>4</sup> Camarero, J. A. New Developments for the Site-Specific Attachment of Protein to Surfaces.  
50  
51 *Biophys. Rev. Lett.* **2006**, *01*, 1-28.  
52  
53  
54  
55  
56  
57  
58  
59  
60

1  
2  
3  
4  
5 <sup>5</sup> Devouge, S.; Conti, J.; Goldsztein, A.; Gosselin, E.; Brans, A.; Voue, M.; De Coninck, J.;  
6  
7 Homble, F.; Goormaghtigh, E.; Marchand-Brynaert, J. Surface Functionalization of Germanium  
8  
9 ATR Devices for Use in FTIR-Biosensors. *J. Colloid Interf. Sci.* **2009**, *332*, 408-415.

10  
11  
12  
13 <sup>6</sup> Schartner, J.; Gavriljuk, K.; Nabers, A.; Weide, P.; Muhler, M.; Gerwert, K.; Kotting, C.  
14  
15 Immobilization of Proteins in their Physiological Active State at Functionalized Thiol Monolayers  
16  
17 on ATR-Germanium Crystals. *Chembiochem* **2014**, *15*, 2529-2534.

18  
19  
20  
21 <sup>7</sup> Goldzstein, A.; Aamouche, A.; Homblé, F.; Voué, M.; Conti, J.; De Coninck, J.; Devouge, S.;  
22  
23 Marchand-Brynaert, J.; Goormaghtigh, E. Ligand–Receptor Interactions in Complex Media: A  
24  
25 New Type of Biosensors for the Detection of Coagulation Factor VIII. *Biosens. Bioelectron.* **2009**,  
26  
27 *24*, 1831-1836.

28  
29  
30  
31 <sup>8</sup> Schartner, J.; Nabers, A.; Budde, B.; Lange, J.; Hoeck, N.; Wiltfang, J.; Kötting, C.; Gerwert,  
32  
33 K. An ATR–FTIR Sensor Unraveling the Drug Intervention of Methylene Blue, Congo Red, and  
34  
35 Berberine on Human Tau and A $\beta$ . *ACS Med. Chem. Lett.* **2017**, *8*, 710-714.

36  
37  
38  
39 <sup>9</sup> Goormaghtigh, E.; Ruyschaert, J.-M.; Raussens, V. Evaluation of the Information Content in  
40  
41 Infrared Spectra for Protein Secondary Structure Determination. *Biophys. J.* **2006**, *90*, 2946-2957.

42  
43  
44  
45 <sup>10</sup> Derenne, A.; Goormaghtigh, E. FTIR Spectroscopy as a Multi-Parameter Analytical Tool.  
46  
47 *Biopharm. Int.* **2017**, *30*, 35-40.

48  
49  
50  
51 <sup>11</sup> Dole, M. N.; Patel, P. A.; Sawant, S. D.; Shedpure, P. S. *Advance Applications of Fourier*  
52  
53 *Transform Infrared Spectroscopy* **2011**, Vol. 7, p 159-166.

1  
2  
3  
4  
5 <sup>12</sup> Ammar, M.; Smadja, C.; Ly, G. T.; Tandjigora, D.; Vigneron, J.; Etcheberry, A.; Taverna, M.;  
6  
7 Dufour-Gergam, E. Chemical Engineering of Self-Assembled Alzheimer's Peptide on a Silanized  
8  
9 Silicon Surface. *Langmuir* **2014**, *30*, 5863-5872.

10  
11  
12  
13 <sup>13</sup> Holmberg, V. C.; Rasch, M. R.; Korgel, B. A. PEGylation of Carboxylic Acid-Functionalized  
14  
15 Germanium Nanowires. *Langmuir* **2010**, *26*, 14241-14246.

16  
17  
18 <sup>14</sup> Nabers, A.; Ollesch, J.; Schartner, J.; Kotting, C.; Genius, J.; Haussmann, U.; Klafki, H.;  
19  
20 Wiltfang, J.; Gerwert, K. An Infrared Sensor Analysing Label-Free the Secondary Structure of the  
21  
22 Abeta Peptide in Presence of Complex Fluids. *J. Biophotonics* **2016**, *9*, 224-234.

23  
24  
25  
26 <sup>15</sup> Voué, M.; Goormaghtigh, E.; Homble, F.; Marchand-Brynaert, J.; Conti, J.; Devouge, S.; De  
27  
28 Coninck, J. Biochemical Interaction Analysis on ATR Devices: a Wet Chemistry Approach for  
29  
30 Surface Functionalization. *Langmuir* **2007**, *23*, 949-955.

31  
32  
33  
34 <sup>16</sup> Pinson, J.; Podvorica, F. Attachment of Organic Layers to Conductive or Semiconductive  
35  
36 Surfaces by Reduction of Diazonium Salts. *Chem. Soc. Rev.* **2005**, *34*, 429-439.

37  
38  
39 <sup>17</sup> Pinson, J. Aryl Diazonium Salts: New Coupling Agents in Polymer and Surface Science.  
40  
41 Chehimi, M. M. *Wiley-VCH: Weinheim* **2012**, pp 1-35.

42  
43  
44 <sup>18</sup> Delamar, M.; Hitmi, R.; Pinson, J.; Saveant, J. M. Covalent Modification of Carbon Surfaces  
45  
46 by Grafting of Functionalized Aryl Radicals Produced from Electrochemical Reduction of  
47  
48 Diazonium Salts. *J. Am. Chem. Soc.* **1992**, *114*, 5883-5884.

49  
50  
51  
52 <sup>19</sup> Collins, G.; Fleming, P.; O'Dwyer, C.; Morris, M. A.; Holmes, J. D. Organic Functionalization  
53  
54 of Germanium Nanowires using Arenediazonium Salts. *Chem. Mater.* **2011**, *23*, 1883-1891.

1  
2  
3  
4  
5       <sup>20</sup> Girard, A.; Geneste, F.; Coulon, N.; Cardinaud, C.; Mohammed-Brahim, T. SiGe  
6  
7 Derivatization by Spontaneous Reduction of Aryl Diazonium Salts. *Appl. Surf. Sci.* **2013**, *282*,  
8  
9 146-155.

10  
11  
12       <sup>21</sup> Lefevre, X.; Segut, O.; Jegou, P.; Palacin, S.; Joussetme, B. Towards Organic Film Passivation  
13  
14 of Germanium Wafers Using Diazonium Salts: Mechanism and Ambient Stability. *Chem. Sci.*  
15  
16 **2012**, *3*, 1662-1671.

17  
18  
19       <sup>22</sup> Combellas, C.; Jiang, D.-e.; Kanoufi, F.; Pinson, J.; Podvorica, F. I. Steric Effects in the  
20  
21 Reaction of Aryl Radicals on Surfaces. *Langmuir* **2009**, *25*, 286-293.

22  
23  
24       <sup>23</sup> Combellas, C.; Kanoufi, F.; Pinson, J.; Podvorica, F. I. Sterically Hindered Diazonium Salts  
25  
26 for the Grafting of a Monolayer on Metals. *J. Am. Chem. Soc.* **2008**, *130*, 8576-8577.

27  
28  
29       <sup>24</sup> Mattiuzzi, A.; Jabin, I.; Mangeney, C.; Roux, C.; Reinaud, O.; Santos, L.; Bergamini, J. F.;  
30  
31 Hapiot, P.; Lagrost, C. Electrografting of Calix[4]arenediazonium Salts to Form Versatile Robust  
32  
33 Platforms for Spatially Controlled Surface Functionalization. *Nat. Commun.* **2012**, *3*, 1130-1138.

34  
35  
36       <sup>25</sup> Troian-Gautier, L.; Valkenier, H.; Mattiuzzi, A.; Jabin, I.; den Brande, N. V.; Mele, B. V.;  
37  
38 Hubert, J.; Reniers, F.; Bruylants, G.; Lagrost, C.; Leroux, Y. Extremely Robust and Post-  
39  
40 Functionalizable Gold Nanoparticles Coated with Calix[4]arenes via Metal-Carbon Bonds. *Chem.*  
41  
42 *Commun.* **2016**, *52*, 10493-10497.

43  
44  
45       <sup>26</sup> Troian-Gautier, L.; Martínez-Tong, D. E.; Hubert, J.; Reniers, F.; Sferrazza, M.; Mattiuzzi,  
46  
47 A.; Lagrost, C.; Jabin, I. Controlled Modification of Polymer Surfaces through Grafting of  
48  
49 Calix[4]arene-Tetradiazoate Salts. *J. Phys. Chem. C* **2016**, *120*, 22936-22945.

1  
2  
3  
4  
5 <sup>27</sup> Santos, L.; Mattiuzzi, A.; Jabin, I.; Vandencastele, N.; Reniers, F.; Reinaud, O.; Hapiot, P.;  
6  
7 Lhenry, S.; Leroux, Y.; Lagrost, C. One-Pot Electrografting of Mixed Monolayers with Controlled  
8  
9 Composition. *J. Phys. Chem. C* **2014**, *118*, 15919-15928.

10  
11  
12  
13 <sup>28</sup> Valkenier, H.; Malytskyi, V.; Blond, P.; Retout, M.; Mattiuzzi, A.; Goole, J.; Raussens, V.;  
14  
15 Jabin, I.; Bruylants, G. Controlled Functionalization of Gold Nanoparticles with Mixtures of  
16  
17 Calix[4]arenes Revealed by Infrared Spectroscopy. *Langmuir* **2017**, *33*, 8253-8260.

18  
19  
20  
21 <sup>29</sup> Yam, C. M.; Deluge, M.; Tang, D.; Kumar, A.; Cai, C. Preparation, Characterization,  
22  
23 Resistance to Protein Adsorption, and Specific Avidin–Biotin Binding of Poly(amidoamine)  
24  
25 Dendrimers Functionalized with Oligo(ethylene glycol) on Gold. *J. Colloid Interf. Sci.* **2006**, *296*,  
26  
27 118-130.

28  
29  
30  
31 <sup>30</sup> Banerjee, I.; Pangule, R. C.; Kane, R. S. Antifouling Coatings: Recent Developments in the  
32  
33 Design of Surfaces That Prevent Fouling by Proteins, Bacteria, and Marine Organisms. *Adv.*  
34  
35 *Mater.* **2011**, *23*, 690-718.

36  
37  
38  
39 <sup>31</sup> Ederth, T.; Ekblad, T.; Pettitt, M. E.; Conlan, S. L.; Du, C.-X.; Callow, M. E.; Callow, J. A.;  
40  
41 Mutton, R.; Clare, A. S.; D'Souza, F.; Donnelly, G.; Bruin, A.; Willemsen, P. R.; Su, X. J.; Wang,  
42  
43 S.; Zhao, Q.; Hederos, M.; Konradsson, P.; Liedberg, B. Resistance of Galactoside-Terminated  
44  
45 Alkanethiol Self-Assembled Monolayers to Marine Fouling Organisms. *ACS Appl. Mater. Inter.*  
46  
47 **2011**, *3*, 3890-3901.

48  
49  
50  
51 <sup>32</sup> Kitano, H.; Kawasaki, A.; Kawasaki, H.; Morokoshi, S. Resistance of Zwitterionic Telomers  
52  
53 Accumulated on Metal Surfaces Against Nonspecific Adsorption of Proteins. *J. Colloid Interf. Sci.*  
54  
55 **2005**, *282*, 340-348.



1  
2  
3  
4  
5 <sup>33</sup> Brady, R. F.; Aronson, C. L. Elastomeric Fluorinated Polyurethane Coatings for Nontoxic  
6 Fouling Control. *Biofouling* **2003**, *19*, 59-62.

7  
8  
9  
10 <sup>34</sup> Li, S.; Yang, D.; Tu, H.; Deng, H.; Du, D.; Zhang, A. Protein Adsorption and Cell Adhesion  
11 Controlled by the Surface Chemistry of Binary Perfluoroalkyl/Oligo(ethylene glycol) Self-  
12 Assembled Monolayers. *J. Colloid Interf. Sci.* **2013**, *402*, 284-290.

13  
14  
15 <sup>35</sup> Harris, J. M. Poly(Ethylene Glycol) Chemistry: Biotechnical and Biomedical Applications.  
16 *Plenum Press: New York* **1992**.

17  
18  
19  
20 <sup>36</sup> Comenge, J.; Puentes, V. F. The Role of PEG Conformation in Mixed Layers: from Protein  
21 Corona Substrate to Steric Stabilization Avoiding Protein Adsorption. *ScienceOpen Research*  
22 **2015**, DOI: 10.14293/S2199-1006.1.SOR-MATSCI.A0Z6OM.v1.

23  
24  
25  
26  
27 <sup>37</sup> Ozcelik, B.; Ho, K. K. K.; Glattauer, V.; Willcox, M.; Kumar, N.; Thissen, H. Poly(ethylene  
28 glycol)-Based Coatings Combining Low-Biofouling and Quorum-Sensing Inhibiting Properties to  
29 Reduce Bacterial Colonization. *ACS Biomater. Sci. Eng.* **2017**, *3*, 78-87.

30  
31  
32  
33  
34  
35  
36  
37  
38 <sup>38</sup> Riedel, T.; Riedelová-Reicheltoová, Z.; Májek, P.; Rodriguez-Emmenegger, C.; Houska, M.;  
39 Dyr, J. E.; Brynda, E. Complete Identification of Proteins Responsible for Human Blood Plasma  
40 Fouling on Poly(ethylene glycol)-Based Surfaces. *Langmuir* **2013**, *29*, 3388-3397.

41  
42  
43  
44  
45  
46  
47  
48 <sup>39</sup> Brash, J. L.; Horbett, T. A. Proteins at Interfaces. In *Proteins at Interfaces II*, American  
49 Chemical Society: **1995**, Vol. 602, pp 1-23.

50  
51  
52  
53  
54  
55  
56  
57  
58  
59  
60 <sup>40</sup> Awadhiya, A.; Tyeb, S.; Rathore, K.; Verma, V. Agarose Bioplastic-Based Drug Delivery  
System for Surgical and Wound Dressings. *Eng. Life Sci.* **2016**, *17*, 204-214.

1  
2  
3  
4  
5 <sup>41</sup> Schartner, J.; Güldenhaupt, J.; Mei, B.; Rögner, M.; Muhler, M.; Gerwert, K.; Kötting, C.  
6  
7 Universal Method for Protein Immobilization on Chemically Functionalized Germanium  
8 Investigated by ATR-FTIR Difference Spectroscopy. *J. Am. Chem. Soc.* **2013**, *135*, 4079-4087.  
9

10  
11  
12 <sup>42</sup> Fairman, C.; Ginges, J. Z.; Lowe, S. B.; Gooding, J. J. Protein Resistance of Surfaces Modified  
13 with Oligo(ethylene glycol) Aryl Diazonium Derivatives. *ChemPhysChem* **2013**, *14*, 2183-2189.  
14

15  
16  
17 <sup>43</sup> Zhao, Y.; Ryu, E.-H. Solvent-Tunable Binding of Hydrophilic and Hydrophobic Guests by  
18 Amphiphilic Molecular Baskets. *J. Org. Chem.* **2005**, *70*, 7585-7591.  
19

20  
21  
22  
23 <sup>44</sup> Griffete, N.; Herbst, F.; Pinson, J.; Ammar, S.; Mangeney, C. Preparation of Water-Soluble  
24 Magnetic Nanocrystals Using Aryl Diazonium Salt Chemistry. *J. Am. Chem. Soc.* **2011**, *133*, 1646-  
25  
26  
27 1649.  
28

29  
30  
31 <sup>45</sup> Doyle, C. D.; Rocha, J.-D. R.; Weisman, R. B.; Tour, J. M. Structure-Dependent Reactivity  
32 of Semiconducting Single-Walled Carbon Nanotubes with Benzenediazonium Salts. *J. Am. Chem.*  
33  
34  
35 *Soc.* **2008**, *130*, 6795-6800.  
36

37  
38  
39 <sup>46</sup> Podvorica, F. I.; Kanoufi, F.; Pinson, J.; Combellas, C. Spontaneous Grafting of Diazoates on  
40 Metals. *Electrochim. Acta* **2009**, *54*, 2164-2170.  
41

42  
43  
44 <sup>47</sup> Amy, S. R.; Chabal, Y. J. Passivation and Characterization of Germanium Surfaces. In  
45 Advanced Gate Stacks for High-Mobility Semiconductors, Dimoulas, A.; Gusev, E.; McIntyre, P.  
46  
47  
48 C.; Heyns, M., Eds. *Springer Berlin Heidelberg: Berlin, Heidelberg*, **2007**, pp 73-113.  
49

50  
51  
52 <sup>48</sup> Chen, Y. W.; Chang, Y.; Lee, R. H.; Li, W. T.; Chinnathambi, A.; Alharbi, S. A.; Hsiue, G.  
53  
54  
55 H. Adjustable Bioadhesive Control of PEGylated Hyperbranch Brushes on Polystyrene Microplate  
56  
57  
58 Interface for the Improved Sensitivity of Human Blood Typing. *Langmuir* **2014**, *30*, 9139-9146.  
59

1  
2  
3  
4  
5 <sup>49</sup> Demirci, S.; Kinali-Demirci, S.; Jiang, S. A Switchable Polymer Brush System for Antifouling  
6 and Controlled Detection. *Chem. Commun.* **2017**, *53*, 3713-3716.  
7  
8  
9  
10  
11  
12  
13  
14  
15  
16

17 **TOC Graphic**

